Graphene Field Effect Transistor Biosensors based on Aptamer for Amyloid-β Detection

Mostafa Salehirozveh, Parisa Dehghani, Milan Zimmermann, Vellaisamy A. L. Roy, and Hadi Heidari

***Abstract*— The development of cost-efficient, sensitive and specific methods to detect amyloid-beta 42 (Aβ42) biomarkers in cerebrospinal fluid and serum-samples is of considerable interest to enable early and reliable diagnosis of Alzheimer's disease as a precondition for future disease-modifying therapies. This paper presents a reduced graphene oxide field effect transistor (r-GO FET) for label free ultrasensitive detection of an Aβ42-biomarker with RNA aptamer. The channel in the device was formed by reduction of graphene oxide nanosheets by self-assembly process. As a result, the interaction between Aβ42 and RNA aptamer on the surface of r-GO channel caused a linear response in the shift of the gate voltage (V_{TG}) where the minimum conductivity occurs. The r-GO FET can detect the biomarker in range of 1ng/ml to 1pg/ml at pH 7.4 with high specificity. The developed r-GO FET is a low-cost, highly sensitive and selective method for detecting tiny concentrations of Aβ42, which would also enable measurements in serum-samples.**

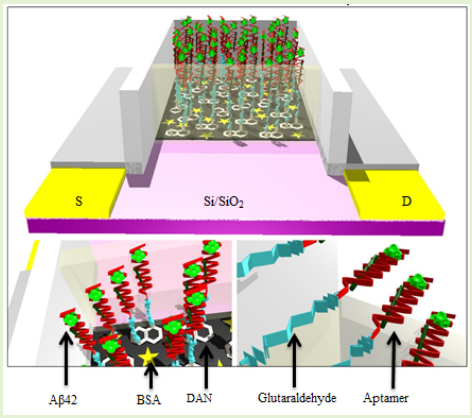

***Index Terms*—Alzheimer's disease, Amyloid beta, RNA, aptamer, label-free detection, bio field-effect transistor, graphene oxide**

I. Introduction

OVER 35 million people around the world suffered from dementia in 2013 [1]. This number is estimated to double every 20 years reaching a value of 65.7 million in 2030, and of 115.4 million in 2050 [2]. The most common cause of senile dementia is the Alzheimer's disease (AD), with currently over 17 million patients worldwide [3]. The AD is often associated with deposition and aggregation of misfolded proteins such as amyloid-beta (Aβ) peptide in brain and forms plaques in the central neural system [4][5][6]. These aggregates can be observed in fibrillar and non-fibrillar forms. Aβ has two isoforms, Aβ40 and Aβ42, which have different rates in spontaneous self-association into oligomers and producing fibrils and plaques [7][8]. Since the generation of Aβ42 aggregates is faster than Aβ40, it can be more neurotoxic [9].

AD diagnostic biosensors *e.g.* semiconductor-based field effect transistor (FET) can miniaturize current bulky and costly hospital-based tools such as Nuclear Magnetic Resonance [10][11], by enabling highly-sensitive technology to identify the specific proteins *e.g.* Aβ40 [12][13][14]. Two-dimensional hexagonal network materials like graphene attract further attention in the field of diagnostic biosensors because of the high mobility of the carrier. For example, detection of proteins by electrochemical graphene biosensors were reported [15][16][17][18][19][20]. Research on Graphene field effect transistor (G-FET) which is based on graphene oxide or reduced graphene oxide has gradually increased in the detection of biomolecules like DNA [21], RNA [22], proteins [23], insulin [24] and bacteria [25][26]. In this context, to improve the performance of G-FET by increasing the mobility of the carrier in a graphene channel, a single layer of graphene is the best candidate [27].

Recognition elements play a key role in a performance of biosensors. Aptamer as a receptor is a short single strand oligonucleotide of DNA or RNA that bind to specific targets. Aptamers offer several advantages like easy to design, cost-efficient to produce, high affinity to targets, and more stable than antibodies [28]. During the past decade, several works of amyloid-binding aptamer have been reported. Ylera *et al.* was reported one of the first works on the design specific RNA aptamer with high affinity to Aβ40 and diagnosed amyloid-peptide as a risk factor in AD [29]. Multiple studies for developing the aptamer against Aβ have been reported based on SELEX and aptamer functionalization like fluorescently tagged anti-Aβ RNA aptamer [30][31][32][33].

This work was partially supported by the UK EPSRC under grant EP/R511705/1, and by the European Union's Horizon 2020 Hybrid Enhanced Regenerative Medicine Systems (HERMES) project (GA n.824164).

M. Salehirozveh is with the Department of Physics and Astronomy, University of Bologna, Bologna, Italy.

P. Dehghani and H. Heidari are with Microelectronics Lab, James Watt School of Engineering, University of Glasgow, G12 8QQ Glasgow, United Kingdom (e-mail: hadi.heidari@glasgow.ac.uk)

M. Zimmermann is with Department of Neurodegenerative Diseases, Hertie Institute for Clinical Brain Research and Center of Neurology, University of Tübingen, and German Center for Neurodegenerative Diseases (DZNE), 72076 Tübingen, Germany.

For exploit r-GO FET in medical application, Debye length is the most considerations parameter, which defines as distance from mobile carriers in r-GO FET channel for screening the surplus charge in the solution. Hence, the charged molecules located out of this distance cannot be detected by the system. Accordingly, the reactions between targets and aptamer should occur within this sensing area. For example, a typical Debye length in 5-10 mM buffer at room temperature is about 5 nm [21]. The r-GO FET biosensors have been exploited for biological application by using DNA [34], enzyme [35] and antibody [17] as a receptor. In this work, we use aptamer (N2), which has a high affinity to bind to the amyloid protein [33].

We aim to develop a cost-efficient, sensitive and specific method for detecting Aβ42 by using a r-GO FET based on RNA aptamer, which was modified on the surface of its channel. Herein, graphene oxide synthesized by modified hummer method and confirmed with atomic force microscopy (AFM) and Fourier-transform infrared spectroscopy (FTIR). After self-assembly of GO on an aminated Si/SiO_2 wafer, RNA aptamers were immobilized on r-GO channel by linkers and characterized by field emission scanning electron microscopy (FESEM) and AFM. Electrical measurements were used to investigate the sensitivity and selectivity of the fabricated device.

II. Materials and methods

A. Materials

Si/SiO2 wafer was obtained from Singapore, graphite powder, 3-aminopropyltriethoxysilane (APTES), 1,5diaminonaphthalene (DAN) and buffer phosphate saline (PBS), Glutaraldehyde, H_2O_2 (30%), ethanolamine, hydrazine monohydrate (85%) purchased from Sigma-Aldrich. sequence of aptamer probe designed by Takapoozist, the sequence of RNA probe is (5'-NH_2-$(CH_2)_4$- UAGCGUAUGCCACUC UCCUGGGACCCCCCGCCGGAUGGCCA-CAUCC-3'. All chemical was of analytical grade and used without high purity nitrogen (99/99% purity) prior to the experiment. DI water was used throughout the work.

Apparatus

AFM images were obtained with VEECO (America) electron microscope. FESEM images were obtained with a Vega_Tescan electron microscopy. FTIR spectroscopic measurements were carried out with a Tensor 27 FT-IR spectrometer (Bruker). All electrochemical measurements were carried out with an Autolab PGSTAT 302N (Eco Chemie, Utrecht, the Netherlands; driven with NOVA software).

Synthesis of GO

GO nanosheets were synthesized by modified Hummer's method [36]. In order to reduce the size of nanosheets and achieve a single layer of GO, sonication was used. In the end, to prepare 1mg/ml concentration of GO and remove the large size of nanosheets, dispersion of GO in DI water was sonicated for 24 hours and centrifuged at 8,000 rpm for 45 min. AFM and FTIR were used to indicate the thickness and qualification of GO nanosheets.

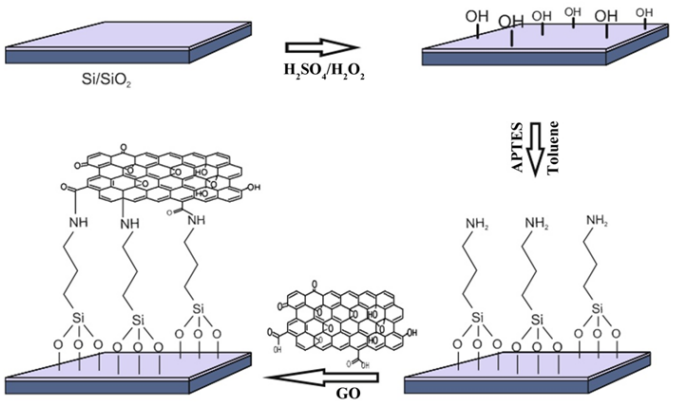

Fig. 1. Schematic formation of a GO on amine-SAM on Si/SiO_2 wafer. Silanization of Si/SiO_2 wafer by APTES after cleaning the surface by piranha solution. Monolayer of silane creates on the surface of substrate. Self-assembly of GO-nanosheets on amine SAM substrate.

B. Fabrication of G-FET device

Fig. 1 shows the schematic steps of a surface modification of graphene FET. The Si/SiO_2 substrate was cleaned by piranha solution ($3H_2SO_4$:$1H_2O_2$) for 20 min, then rinsed with DI water and toluene. The Si/SiO_2 wafer was silanized with 0.1% (v/v) APTES in anhydrous toluene for 4 hours [37]. After silanization, the remaining APTES molecules were washed with toluene to organize self-assembled monolayer of ATPES [38]. Then, the aminated Si/SiO_2 wafer was immersed into GO dispersion for 6 h. After that, GO nanosheets were strongly bound to the aminated substrate. At last, the self-assemble of GO nanosheets on the surface of the aminated substrate was reduced by hydrazine vapor for 18 h at 50 °C and heated at 220 °C for 12 h to produce r-GO.

Fig. 2 illustrates the fabrication steps of the proposed r-GO FET. The Au source and drain (S/D) electrodes and Al_2O_3, which was capping the electrodes in order to barricade interaction of biomolecules to Au S/D were formed by thermal evaporating on r-GO layer using metal shadow mask on substrate. The width and length of r-GO channel which is located between the S/D electrodes are 40 µm and 3.2 mm respectively. Au electrodes were coated on the substrate by sputtering and using a metal mask to pattern and the PDMS layer was directly pasted on the Al_2O_3 capped S/D electrodes to remove the electrode-electrolyte leakage. Encapsulation of the electrode area by two Al_2O_3 and PDMS layers was important to keep level of the leakage current between gate and source electrodes undetectable during electrical measurements. At last, in order to isolate and seal the channel, acrylic fixture with the length of 4 mm, the height of 100 µm and width of 200 µm was used and top gate was located at top of the fixture that is in contact with the analyte which is illustrated in Fig. 3a. Here, for transport the Aβ solution, two syringes were designed at top of the fixture as input and output pump to circulate the sample solution through the channel, as shown in Fig. 3.

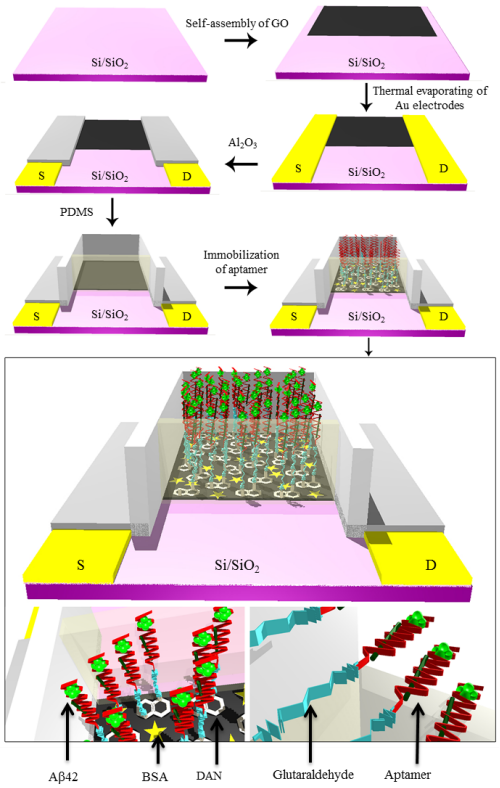

Fig. 2. Schematic of r-GO FET device fabrication and detection of Aβ-Aptamer complex. Formation of Au S/D electrode, covering the electrode by Al_2O_3 and using PDMS layers to isolate the device. Functionalization of channel by DAN and glutaraldehyde and immobilization of Aptamer to linkers on surface of r-GO channel and blocking the surface by BSA for non-specific binding.

C. Immobilization of Aptamer

RNA aptamer oligonucleotide of Alzheimer with 5' amino modification was synthesized by Takapoozist. The base sequence: (5'-UAGCGUAUGCCACUCUCCUGGGA CCCCCCGCCGGAUGGCCA-CAUCC-3'). For preparing 100 µM concentration, the aptamer was dissolved in 100 mM phosphate-buffered saline (PBS) (pH 7.4). The aptamer was immobilized on r-GO to work as a receptor for Aβ42 by using 1,5diaminonaphthalene (DAN) and glutaraldehyde linkers.

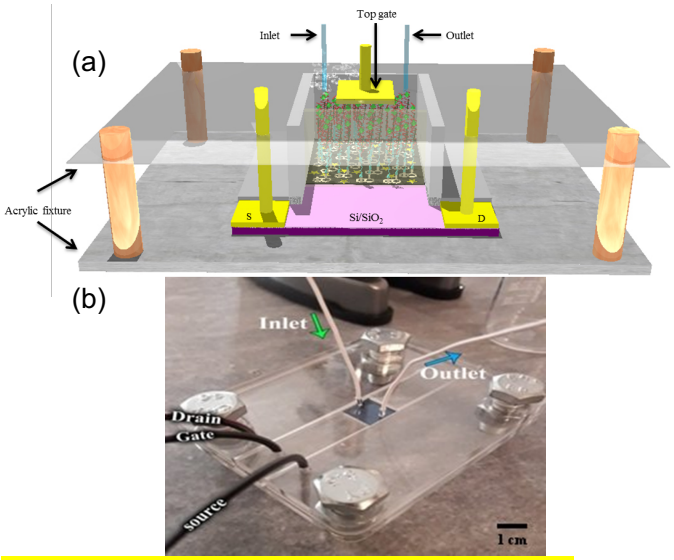

Fig. 3. (a) Schematic and (b) optical images of acrylic fixture.

The Polydimethylsiloxane (PDMS) well was filled with 100 µM DAN in 40 µL methanol for 1 h. Then it was rinsed with methanol and DI water. The DAN component was bound to r-GO by π-π stacking between a network of r-GO and a pyrenyl group. 20 µL of 2% glutaraldehyde in PBS (pH 7) was used for conjugating to DAN for 2 h and then washed with PBS. The well was incubated with 100 nM of Alzheimer aptamer in PBS in pH 7 for 15 h at room temperature. After the incubation, the substrate was washed with PBS at pH 7. The transfer curve of r-GO FET was observed after immobilization (Fig. 8).

After immobilization of aptamer and introducing Aβ42, AFM and FESEM were used to confirm the processes.

D. Blocking the surface of r-GO for specific detection

After immobilization of aptamers on the surface of r-GO, bare areas that were not covered with receptors were blocked by immersing the substrate in 10 µg/ml bovine serum albumin (BSA) solution for 10 min at 4 °C in order to prevent non-specific attachment of targets with the bare surface.

E. Aptamer sensing characteristic

Electrical measurements were performed by observing the changes in drain current while different concentration of Aβ42 in PBS (10mM Na_2HPO_4 and 10mM NaH_2PO_4) from 1ng/ml to 1pg/ml were injected. Voltage was applied to the reference electrode.

Aβ42 was prepared with 20 mM NaOH to a final concentration of 0.5 mM. The solution was then sonicated for

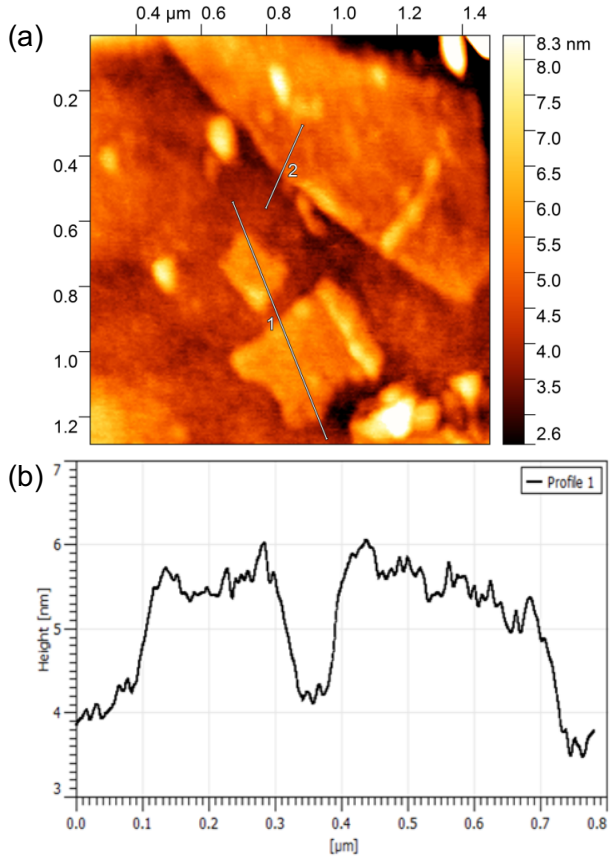

Fig. 4. (a) Typical AFM image of GO, and (b) height profile of single to bi-layer of GO nanosheet.

1 min and kept at room temperature for 5 min to completely dissolved the sample. This was followed by centrifuging at 13,000 rpm for 20 min to remove any aggregates that might have formed in the solution. The supernatant was used as the stock solution. Prior to each experiment, aliquots of the 0.5 mM stock solution were diluted with 10 mM phosphate buffer (pH 7.4) to 25 µM [39].

III. RESULTS AND DISCUSSION

A. Characterization of GO

Nanosheets of GO were visualized by AFM. Fig. 4a depicts the typical image of GO and Fig. 4b shows the thickness of GO sheets. The thickness of GO sheets were in a rage of 1.3–1.7 nm, which indicates the presence of hydroxyl, epoxy and carboxyl groups on surface and side of GO sheets and the existence of single to bi-layer of GO [40][41][42][43].

FTIR analysis of GO (Fig.5) shows the following characteristic peaks of functional groups. Stretching peak for C-O-C (~1060 cm^{-1}), vibration peaks for C-O (~1185 cm^{-1}) and C=C (~1618 cm^{-1}), bending vibration peaks for O-H (~1370 cm^{-1}) and stretching vibration for C=O (~1720 cm^{-1}), and O-H (3200-3500 cm^{-1}), which is about residual water between GO sheets and hydroxyl and carboxyl groups of GO nanosheets. The results demonstrates the large amounts of oxygen-containing groups exposed on the surface of GO [44][45][46].

B. Characterization of the modified r-GO channel

First, we functionalized the r-GO by DAN and glutaraldehyde as linkers. Then topography from the surface of the r-GO channel was analyzed by AFM after immobilization of Alzheimer aptamer and adding Aβ42. As shown in Fig.6, AFM results demonstrate immobilization of aptamer on the surface of the modified r-GO channel with a room-mean-squared (RMS) roughness of 1.7 nm. After adding Aβ42 the RMS was 4.68 nm. The small spots in the illustration demonstrate the high density of aptamer-binding to the r-GO channel.

In order to confirm the immobilization of aptamer on the surface of r-GO channel, FESEM was used. The results from aptamer immobilization indicate densely distributed Alzheimer aptamer on the r-GO channel (Fig. 7a). Fig. 7b and 7c show the middle of the r-GO channel and the edge of electrode respectively. As shown in figure 7c, the upper and

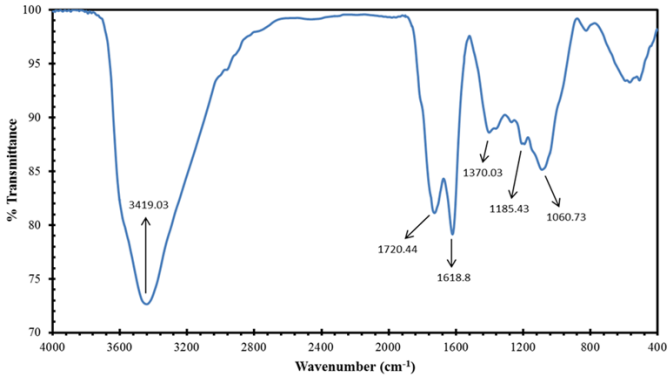

Fig. 5. FTIR spectra of GO.

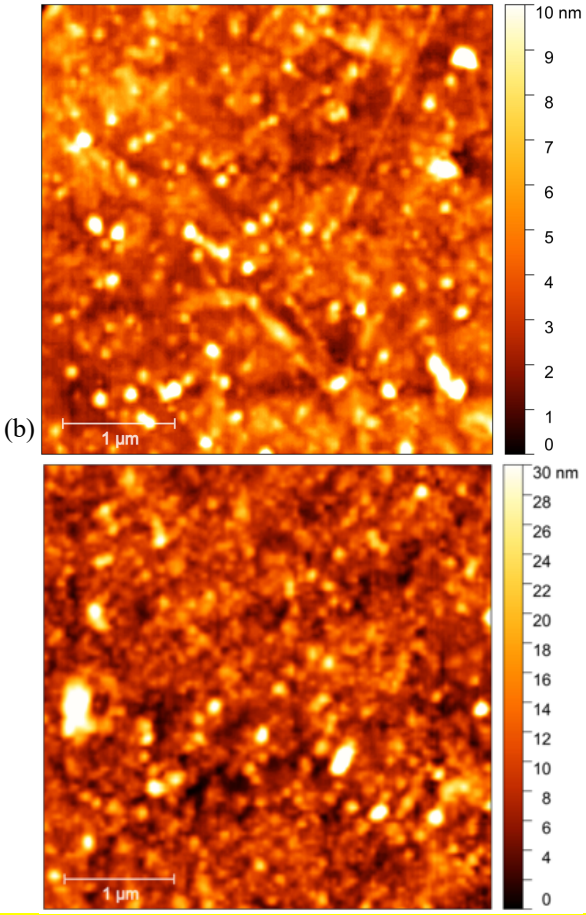

Fig. 6. AFM images of channel modified with aptamer and Aβ42. (a) Topography from the surface after immobilization of aptamer and (b) introducing Aβ42.

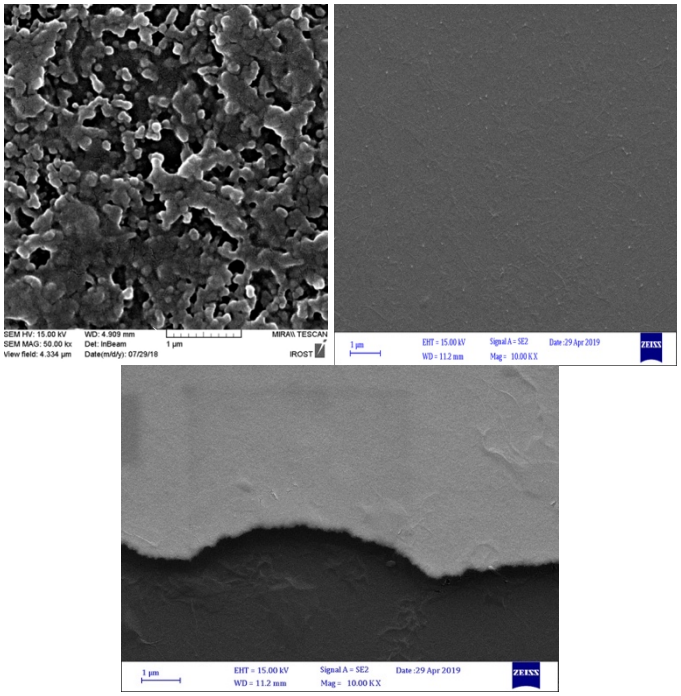

Fig. 7. FESEM images of showing immobilization of aptamer on modified r-GO. (a) Aptamers were densely assembled on surface of channel. (b) Image from show the middle of the r-GO channel and (c) from the electrode's edge that the upper part of image is Au electrode and the downside is a r-GO channel.

lighter part of the image is Au electrode and the other dark side is an r-GO channel.

C. Protein detection

The effect of Alzheimer aptamer immobilization on the surface of r-GO channel was investigated by electrical measurements. Fig. 8 shows the transfer curve of the drain current (I_D) versus top gate voltage (V_{TGS}) of bare r-GO FET (black line) in comparison to r-GO FET (red line) with immobilized aptamer at a drain voltage (V_D) of 10 mV in PBS. As shown in Fig. 8, I_D increased after immobilization. This results from an increase in density of negative charge due to binding of aptamer on the r-GO channel. This indicates the successful immobilization of Alzheimer aptamer on the surface of the r-GO channel. It should be noted that the same slope of I_D- V_{TGS} curves express no defects were presented on the surface of r-GO by immobilization.

The transfer curves of aptamer-modified r-GO FET in response to the different concentrations of Aβ42 ranging from 1ng/ml to 1pg/ml at a drain voltage (V_D) of 70 mV in PBS depicted in Fig. 9. The positive shift of the transfer curve is due to the negative charge of Aβ42 (pI=5.5), which induces p-doping to aptamer-modified r-GO FET. On the other hand,

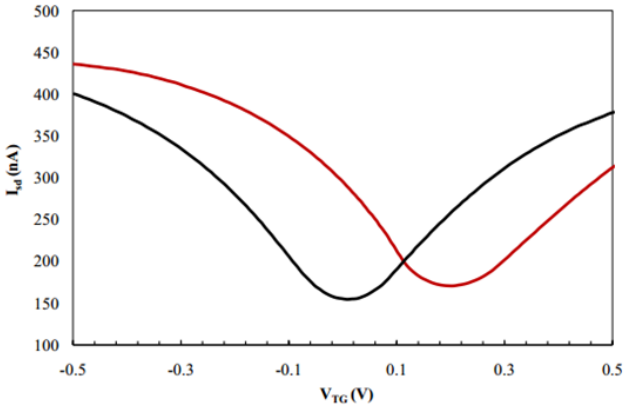

Fig. 8. Transfer curve, before and after modifying r-GO with aptamer. The black demonstrates the drain current (I_D) versus top gate voltage (V_{TGS}) of bare r-GO FET and the red line belongs to r-GO FET after immobilization of aptamer.

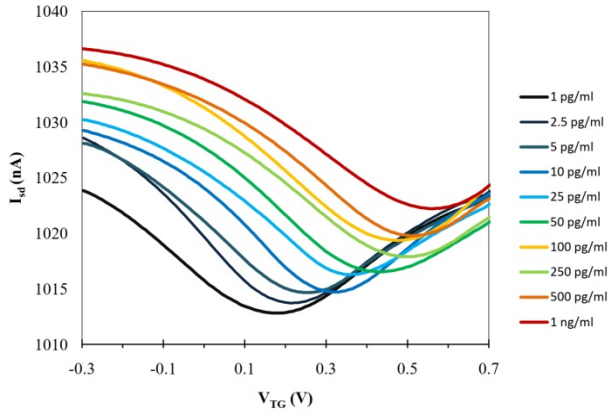

Fig. 9. Detection of Aβ42 aggregation by aptamer-modified r-GO FET. The change of transfer curve of aptamer-modified r-GO FET were recorded for 4h by introducing different concentration of Aβ42 solution at pH 7.4. The gradual aggregation of the negatively charged Aβ42 (pI=5.5) induced a p-doping to aptamer-modified r-GO FET.

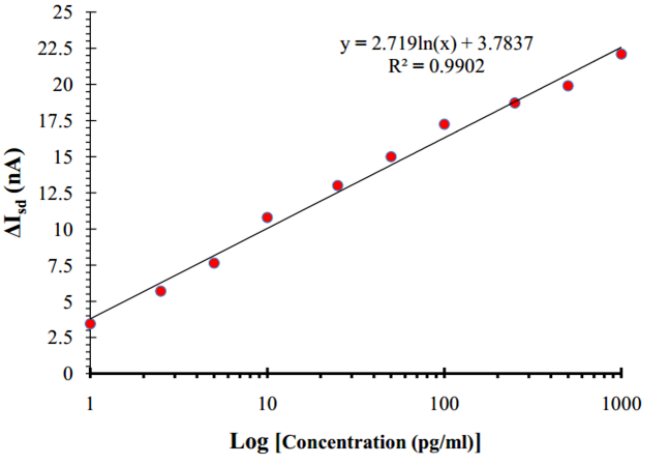

Fig. 10. Calibration curve of drain current as a function of different concentration of Aβ42.

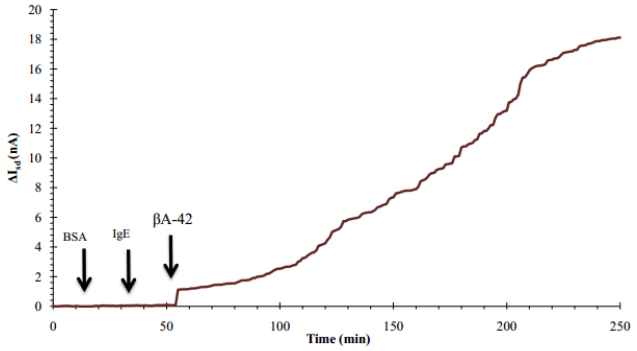

Fig. 11. The course time of normalized I_D for r-GO FET with aptamer-modified channel. 100 pg/ml of BSA, IgE and Aβ42 in buffer phosphate at pH 7.4 were injected on to the aptamer-modified channel for 4h.

interaction between aptamer and Aβ42 within the Debye Length, caused an increase in current because of the change in electrical composition of electrolyte after adding the Aβ42. Fig. 10 shows the calibration curve representing the relationship between the drain current on the one hand and the concentration of Aβ42 on the other hand. The upper detection limit was reduced from 1ng/ml to 1 pg/ml. It should be mentioned that, because of the formation of layer of Aβ42 fibril during 4h and near-full coverage of the channel surface due to the hydrogen bonding occurred between protofibril and fibril [47][48][49], the decreasing in ion permeation through this protein layer was occurred that leaded to reduce in gate capacitance [48]. Also, this formation of the Aβ42 layer, chemical structure of r-GO that consists of unreduced, covalently bonded oxygen groups, and absorbed BSA on r-GO, caused small reduction in mobility of carriers in a r-GO channel [48][50][51]. Therefore, the measurement was performed at V_D of 70 mV to achieve the highest sensitivity and limit of detection in these ranges of concentrations.

To investigate the specificity of the aptamer-modified r-GO FET, different proteins were added. Fig. 11 shows the time course of normalized I_D for aptamer-modified r-GO FET. 100 pg/ml BSA, IgE and Aβ42 were added to the aptamer-modified channel for 4h. I_D slightly increased after adding BSA. On the other hand, I_D decreased slightly after adding IgE. Fig. 11 shows a significant increase in I_D after adding Aβ42. The discrepancy in the drain current change can be

explained by the difference in the isoelectric point of these proteins. The isoelectric points of BSA and Aβ42 are 5.3 and 5.5, respectively, which indicate that both proteins are negatively charged in phosphate-buffer solution at pH 7.4. The isoelectric point of IgE is 6.5~9.5. Since the I_D decreased after adding the IgE molecules. Therefore, the results indicate that the Aptamer-modified r-GO FET was successfully responded to the Aβ42 specifically. All in all, this bio-FET can detect extremely small quantities of Aβ42 with high specificity.

IV. Conclusion

We could develop a (1) cost efficient method for detecting (2) small concentrations of Aβ ranging from 1ng/ml to 1pg/ml with (3) high specificity. Currently, diagnosis of Alzheimer´s disease is supported by measurement of decreased CSF-concentrations of Aβ42 in CSF and increased concentrations of h-TAU and p-TAU in CSF by methods like ELISA. The sensitivity of the commercial ELISA is in the range of pM, while our device had a wide dynamic range from 1ng/ml to 1pg/ml [52][53][54]. Several research groups tried to also measure Aß42 in plasma samples, which would be a faster and easier way with also more acceptance from the patient´s point of view including immunoassay and xMAP [53][55]. Another prerequisite is a high specificity of such a method since there are a lot of plasma proteins leading to possible false positive results when also resulting into a detection signal or even to false negative results when preventing the binding of amyloid-proteins. We could detect very small concentrations of Aβ42 in a range of 1ng/ml to 1pg/ml with our reduced graphene oxide field effect transistor-method. Adding BSA or IgG did not lead to a significant change in drain current, too, thus enabling potential measurements in plasma samples with a high specificity.

As future work, we cover the limitation of this study and link it with clinical and imaging data. All in all, our new method might help to improve early diagnosis of Aβ pathology as a very important requirement for future disease-modifying therapies or other medical drugs since this enables an early begin of therapy.

References

[1] T. Cumming and A. Brodtmann, "Dementia and stroke: the present and future epidemic," *Int. J. Stroke*, vol. 5, no. 6, pp. 453–454, 2010.

[2] A. Gulland, "Number of people with dementia will reach 65.7 million by 2030, says report." British Medical Journal Publishing Group, 2012.

[3] D. E. Barnes and K. Yaffe, "The projected effect of risk factor reduction on Alzheimer's disease prevalence," *Lancet Neurol.*, vol. 10, no. 9, pp. 819–828, 2011.

[4] J. Ghiso and B. Frangione, "Amyloidosis and Alzheimer's disease," *Adv. Drug Deliv. Rev.*, vol. 54, no. 12, pp. 1539–1551, 2002.

[5] A. Mathew, Y. Yoshida, T. Maekawa, and D. S. Kumar, "Alzheimer's disease: Cholesterol a menace?," *Brain Res. Bull.*, vol. 86, no. 1–2, pp. 1–12, 2011.

[6] K. G. Mawuenyega *et al.*, "Decreased clearance of CNS β-amyloid in Alzheimer's disease," *Science (80-.).*, vol. 330, no. 6012, p. 1774, 2010.

[7] P. E. Spies *et al.*, "The cerebrospinal fluid amyloid β42/40 ratio in the differentiation of alzheimer's disease from non-alzheimer's dementia," *Curr. Alzheimer Res.*, vol. 7, no. 5, pp. 470–476, 2010.

[8] M. Wogulis, S. Wright, D. Cunningham, T. Chilcote, K. Powell, and R. E. Rydel, "Nucleation-dependent polymerization is an essential component of amyloid-mediated neuronal cell death," *J. Neurosci.*, vol. 25, no. 5, pp. 1071–1080, 2005.

[9] A. R. Simard, *et al.*, "Bone marrow-derived microglia play a critical role in restricting senile plaque formation in Alzheimer's disease," *Neuron*, vol. 49, no. 4, pp. 489–502, 2006.

[10] K.-M. Lei, H. Heidari, P.-I. Mak, M.-K. Law, F. Maloberti, and R. P. Martins, "A handheld high-sensitivity micro-NMR CMOS platform with B-field stabilization for multi-type biological/chemical assays," *IEEE J. Solid-State Circuits*, vol. 52, no. 1, pp. 284–297, 2016.

[11] V. Nabaei, R. Chandrawati, and H. Heidari, "Magnetic biosensors: Modelling and simulation," *Biosens. Bioelectron.*, vol. 103, pp. 69–86, 2018.

[12] M. Abe *et al.*, "Quantitative detection of protein using a top-gate carbon nanotube field effect transistor," *J. Phys. Chem. C*, vol. 111, no. 24, pp. 8667–8670, 2007.

[13] K. Maehashi, T. Katsura, K. Kerman, Y. Takamura, K. Matsumoto, and E. Tamiya, "Label-free protein biosensor based on aptamer-modified carbon nanotube field-effect transistors," *Anal. Chem.*, vol. 79, no. 2, pp. 782–787, 2007.

[14] M. T. Martínez, *et al.*, "Label-free DNA biosensors based on functionalized carbon nanotube field effect transistors," *Nano Lett.*, vol. 9, no. 2, pp. 530–536, 2009.

[15] P. Bollella *et al.*, "Beyond graphene: electrochemical sensors and biosensors for biomarkers detection," *Biosens. Bioelectron.*, vol. 89, pp. 152–166, 2017.

[16] D. Du, S. Guo, L. Tang, Y. Ning, Q. Yao, and G.-J. Zhang, "Graphene-modified electrode for DNA detection via PNA–DNA hybridization," *Sensors Actuators B Chem.*, vol. 186, pp. 563–570, 2013.

[17] F. Liu, Y. H. Kim, D. S. Cheon, and T. S. Seo, "Micropatterned reduced graphene oxide based field-effect transistor for real-time virus detection," *Sensors Actuators B Chem.*, vol. 186, pp. 252–257, 2013.

[18] L.-H. Pan, S.-H. Kuo, T.-Y. Lin, C.-W. Lin, P.-Y. Fang, and H.-W. Yang, "An electrochemical biosensor to simultaneously detect VEGF and PSA for early prostate cancer diagnosis based on graphene oxide/ssDNA/PLLA nanoparticles," *Biosens. Bioelectron.*, vol. 89, pp. 598–605, 2017.

[19] W. Sun *et al.*, "Electrochemical DNA biosensor based on partially reduced graphene oxide modified carbon ionic liquid electrode for the detection of transgenic soybean A2704-12 gene sequence," *Electroanalysis*, vol. 25, no. 6, pp. 1417–1424, 2013.

[20] H. Teymourian, A. Salimi, and S. Khezrian, "Fe3O4 magnetic nanoparticles/reduced graphene oxide nanosheets as a novel electrochemical and bioeletrochemical sensing platform," *Biosens. Bioelectron.*, vol. 49, pp. 1–8, 2013.

[21] Y. Ohno, K. Maehashi, and K. Matsumoto, "Label-free biosensors based on aptamer-modified graphene field-effect transistors," *J. Am. Chem. Soc.*, vol. 132, no. 51, pp. 18012–18013, 2010.

[22] M. Tian *et al.*, "RNA detection based on graphene field-effect transistor biosensor," *Adv. Condens. Matter Phys.*, vol. 2018, 2018.

[23] Y. Ohno, K. Maehashi, K. Inoue, and K. Matsumoto, "Label-free aptamer-based immunoglobulin sensors using graphene field-effect transistors," *Jpn. J. Appl. Phys.*, vol. 50, no. 7R, p. 70120, 2011.

[24] Z. Hao *et al.*, "Real-time monitoring of insulin using a graphene field-effect transistor aptameric nanosensor," *ACS Appl. Mater. Interfaces*, vol. 9, no. 33, pp. 27504–27511, 2017.

[25] G. Wu *et al.*, "Graphene Field-Effect Transistors for the Sensitive and Selective Detection of Escherichia coli Using Pyrene-Tagged DNA Aptamer," *Adv. Healthc. Mater.*, vol. 6, no. 19, p. 1700736, 2017.

[26] G. Wu, M. Meyyappan, and K. W. C. Lai, "Simulation of graphene field-effect transistor biosensors for bacterial detection," *Sensors*, vol. 18, no. 6, p. 1715, 2018.

[27] K. Nagashio, T. Nishimura, K. Kita, and A. Toriumi, "Mobility variations in mono-and multi-layer graphene films," *Appl. Phys. express*, vol. 2, no. 2, p. 25003, 2009.

[28] S. Klussmann, *The aptamer handbook: functional oligonucleotides and their applications*. John Wiley & Sons, 2006.

[29] F. Ylera, R. Lurz, V. A. Erdmann, and J. P. Fürste, "Selection of RNA aptamers to the Alzheimer's disease amyloid peptide," *Biochem. Biophys. Res. Commun.*, vol. 290, no. 5, pp. 1583–1588, 2002.

[30] M. Chakravarthy *et al.*, "Development of DNA aptamers targeting low-molecular-weight amyloid-β peptide aggregates in vitro," *Chem. Commun.*, vol. 54, no. 36, pp. 4593–4596, 2018.

[31] C. T. Farrar, C. M. William, E. Hudry, T. Hashimoto, and B. T. Hyman, "RNA aptamer probes as optical imaging agents for the detection of amyloid plaques," *PLoS One*, vol. 9, no. 2, 2014.

[32] F. Rahimi, "Aptamers Selected for Recognizing Amyloid β-Protein—A Case for Cautious Optimism," *Int. J. Mol. Sci.*, vol. 19, no. 3, p. 668, 2018.
[33] T. Takahashi, K. Tada, and H. Mihara, "RNA aptamers selected against amyloid β-peptide (Aβ) inhibit the aggregation of Aβ," *Mol. Biosyst.*, vol. 5, no. 9, pp. 986–991, 2009.
[34] B. Cai, S. Wang, L. Huang, Y. Ning, Z. Zhang, and G.-J. Zhang, "Ultrasensitive label-free detection of PNA–DNA hybridization by reduced graphene oxide field-effect transistor biosensor," *ACS Nano*, vol. 8, no. 3, pp. 2632–2638, 2014.
[35] E. Piccinini, C. Bliem, C. Reiner-Rozman, F. Battaglini, O. Azzaroni, and W. Knoll, "Enzyme-polyelectrolyte multilayer assemblies on reduced graphene oxide field-effect transistors for biosensing applications," *Biosens. Bioelectron.*, vol. 92, pp. 661–667, 2017.
[36] S. Park and R. S. Ruoff, "Chemical methods for the production of graphenes," *Nat. Nanotechnol.*, vol. 4, no. 4, p. 217, 2009.
[37] K. De Vos, I. Bartolozzi, E. Schacht, P. Bienstman, and R. Baets, "Silicon-on-Insulator microring resonator for sensitive and label-free biosensing," *Opt. Express*, vol. 15, no. 12, pp. 7610–7615, 2007.
[38] T. Bronder, C. S. Wu, A. Poghossian, C. F. Werner, M. Keusgen, and M. J. Schöning, "Label-free detection of DNA hybridization with light-addressable potentiometric sensors: comparison of various DNA-immobilization strategies," *Procedia Eng.*, vol. 87, pp. 755–758, 2014.
[39] Y. Fezoui *et al.*, "An improved method of preparing the amyloid β-protein for fibrillogenesis and neurotoxicity experiments," *Amyloid*, vol. 7, no. 3, pp. 166–178, 2000.
[40] Q. Lyu, H. Yan, L. Li, Z. Chen, H. Yao, and Y. Nie, "Imidazolium ionic liquid modified graphene oxide: as a reinforcing filler and catalyst in epoxy resin," *Polymers (Basel).*, vol. 9, no. 9, p. 447, 2017.
[41] S. Stankovich *et al.*, "Graphene-based composite materials," *Nature*, vol. 442, no. 7100, pp. 282–286, 2006.
[42] J. Xu, M. Xu, J. Wu, H. Wu, W.-H. Zhang, and Y.-X. Li, "Graphene oxide immobilized with ionic liquids: Facile preparation and efficient catalysis for solvent-free cycloaddition of CO 2 to propylene carbonate," *RSC Adv.*, vol. 5, no. 88, pp. 72361–72368, 2015.
[43] C. Zhu, S. Guo, Y. Fang, and S. Dong, "Reducing sugar: new functional molecules for the green synthesis of graphene nanosheets," *ACS Nano*, vol. 4, no. 4, pp. 2429–2437, 2010.
[44] S. Eigler, C. Dotzer, A. Hirsch, M. Enzelberger, and P. Müller, "Formation and decomposition of CO2 intercalated graphene oxide," *Chem. Mater.*, vol. 24, no. 7, pp. 1276–1282, 2012.
[45] D. C. Marcano *et al.*, "Improved synthesis of graphene oxide," *ACS Nano*, vol. 4, no. 8, pp. 4806–4814, 2010.
[46] Y. Xu, H. Bai, G. Lu, C. Li, and G. Shi, "Flexible graphene films via the filtration of water-soluble noncovalent functionalized graphene sheets," *J. Am. Chem. Soc.*, vol. 130, no. 18, pp. 5856–5857, 2008.
[47] S. I. A. Cohen *et al.*, "Proliferation of amyloid-β42 aggregates occurs through a secondary nucleation mechanism," *Proc. Natl. Acad. Sci.*, vol. 110, no. 24, pp. 9758–9763, 2013.
[48] I. Heller, A. M. Janssens, J. Männik, E. D. Minot, S. G. Lemay, and C. Dekker, "Identifying the mechanism of biosensing with carbon nanotube transistors," *Nano Lett.*, vol. 8, no. 2, pp. 591–595, 2008.
[49] L. C. Serpell, "Alzheimer's amyloid fibrils: structure and assembly," *Biochim. Biophys. Acta (BBA)-Molecular Basis Dis.*, vol. 1502, no. 1, pp. 16–30, 2000.
[50] T. S. Sreeprasad and V. Berry, "How do the electrical properties of graphene change with its functionalization?," *Small*, vol. 9, no. 3, pp. 341–350, 2013.
[51] H. Zhang, Z. Zhu, Y. Wang, Z. Fei, and J. Cao, "Changing the activities and structures of bovine serum albumin bound to graphene oxide," *Appl. Surf. Sci.*, vol. 427, pp. 1019–1029, 2018.
[52] M. Fiorini, M. Bongianni, M. D. Benedetti, S. Monaco, and G. Zanusso, "Reappraisal of Aβ 40 and Aβ 42 Peptides Measurements in Cerebrospinal Fluid of Patients with Alzheimer's Disease," *J. Alzheimer's Dis.*, vol. 66, no. 1, pp. 219–227, 2018.
[53] P. Lewczuk *et al.*, "Cerebrospinal Fluid Aβ 42/40 Corresponds Better than Aβ 42 to Amyloid PET in Alzheimer's Disease," *J. Alzheimer's Dis.*, vol. 55, no. 2, pp. 813–822, 2017.
[54] B. Reddy, "Nanoscale BioFETs for ultrasensitive pH and biomolecular detection." University of Illinois at Urbana-Champaign, 2012.
[55] P. Mehta, M. deLeon, K. Blenow, W. Zigman, and H. Zetterberg, "Diagnostic Accuracy of ELISA and Luminex Technology (xMAP) for the Quantitation of CSF Amyloid Beta 40 and 42 Peptides to differentiate Patients with Probable Alzheimer Disease (AD) from Elderly Non-demented Controls (P1. 094)." AAN Enterprises, 2017.

Mostafa Salehirozveh is a PhD student at Department of Physics of the University of Bologna, Italy, working on Pico Potentiostat for Nano-Electrochemical Measurements. He completed his master's degree in field of Nanomaterial Nanotechnology at University of Isfahan. He is passionate about physics of semiconductors, CMOS microchip, MEMS and NEMS (micro-electromechanical systems and nano-electromechanical systems), Bio-FETs and Biosensors, Single-entity electrochemistry (SEE). In these fields he has experienced on near 10 projects. He is a first author of three articles which were submitted in high impacted journals.

Parisa Dehghani awarded her master's degree from Isfahan University in field of Nanobiotechnology and bachelor's degree from Shiraz University, Iran. Her main research interest is Biosensors. She starts her PhD on developing Bio-FET sensors at the University of Glasgow, United Kingdom, from October 2020. She is author/co-author of 5 journal articles and one book chapter of "Neural Regenerative Nanomedicine" book by the Elsevier. She has presentations in 10 conferences and workshops.

Milan Zimmerman was born in Frankfurt a.M., Germany in 1990. He studied medicine at the Charité Universitätsmedizin Berlin and completed his medical examination in 2016. He received his MD degree also from the medical university in Berlin in 2017.
Since 2016, he works as a resident and scientist at the medical university in Tuebingen, Germany, the Hertie institute for clinical brain research and the German center for neurodegenerative diseases. His main research interests include neurodegenerative diseases with focus on Parkinson´s disease and dementia. He is author of 10 articles in peer-reviewed medical journals.

Roy Vellaisamy is a Professor of Intelligent systems at the James Watt School of Engineering, University of Glasgow. He works on multidisciplinary research blending device physics with materials chemistry and electronic engineering. He has published over 200 articles in journals such as Nature Communications, Advanced Materials, Advanced Functional Materials, Analytical Chemistry etc. and his publications are cited over 7500 times [h-index - 42]. He has 21 US/International/Chinese patents. Recently, he received gold medal for his "Sensor Platform" at the International Exhibition of Inventions Geneva 2019.

Hadi Heidari (S'11–M'15–SM'17) is an Assistant Professor (Lecturer) in the James Watt School of Engineering and lead of the Microelectronics Lab (meLAB) at the University of Glasgow, United Kingdom. He has authored over 150 articles in top-tier peer reviewed journals and in international conferences. He is the General Chair of 27th IEEE ICECS 2020, an IEEE Senior Member, and an Editor for the Microelectronics Journal. He is member of the IEEE Circuits and Systems Society Board of Governors (BoG), and Member-at-Large IEEE Sensors Council. He has been the recipient of a number of awards including the 2019 IEEE Sensors Council Young Professional Award, the Rewards for Excellence prize from the University of Glasgow (2018), Best Paper Award from the IEEE ISCAS'14 conference, Gold Leaf Award from the IEEE PRIME'14 Conference.